The network structure of the merit function space of EUV mirror systems

Oana Marinescu* and Florian Bociort
Optics Research Group, Delft University of Technology
Lorentzweg 1, 2628 CJ Delft, The Netherlands

ABSTRACT

The merit function space of mirror systems for EUV lithography is studied. Local minima situated in a multidimensional merit function space are connected via links that contain saddle points and form a network. In this work we present the first networks for EUV lithographic objectives and discuss how these networks change when control parameters, such as aperture and field are varied and constraints are used to limit the variation domain of the variables. A good solution in a network obtained with a limited number of variables has been locally optimized with all variables to meet practical requirements.

Keywords: network, saddle point, optical system design, EUV lithography, optimization

1. INTRODUCTION

Finding good local minima in multidimensional merit function spaces is a difficult task, because of the large number of existing solutions. Commercial optical design programs use nowadays global optimization algorithms, such as global synthesis[1], global explorer[2], simulated annealing[3] and genetic algorithms[4]. However, they give the solutions as single points in the merit function space without any information about the relations between them.

It has been shown recently[5] that the local minima situated in a multidimensional merit function space are connected via optimization paths that start from a special type of saddle point (saddle point with Morse index 1) and form a network. Examples of the network structure for the Double Gauss and the Cooke Triplet have also been given[5-7]. In this article, we give examples of networks for the merit function space of complex mirror systems used in extreme-ultraviolet (EUV) lithography.

We first give a brief description of the global optimization method based on network search[6]. Then we present network graphs of the merit function space of a six-mirror EUV system with six variables. We discuss how variations of the control parameters, such as numerical aperture and field, and changes of the constraints influence these networks. A good six-mirror configuration, generated by our global optimization method, is then locally optimized using all variables for practical demands.

2. SADDLE POINTS

In the neighborhood of a critical point (i.e. a point at which the gradient of F vanishes), the merit function F is given by:

$$F(x_1, x_2, ..., x_N) = F_0 + \sum H_{ij} x_i x_j \qquad (1)$$

* o.marinescu@tnw.tudelft.nl; phone: +31 15 278 8109; fax +31 15 278 8105;
http://wwwoptica.tn.tudelft.nl/users/bociort/networks.html

Current Developments in Lens Design and Optical Engineering VI,
edited by Pantazis Zakos Mouroulis, Warren J. Smith, R. Barry Johnson,
Proceedings of SPIE Vol. 5874 (SPIE, Bellingham, WA, 2005) · 0277-786X/05/$15

where F_0 is the value of F at the critical point and x_i are the optimization variables, with the origin of the coordinate system at the critical point.

At a critical point for which the determinant of the matrix

$$H_{ij} = \frac{1}{2}\frac{\partial^2 F}{\partial x_i \partial x_j} \tag{2}$$

is non-zero the coordinate system can be rotated so that Eq. (1) contains only squares of the variables.

$$F(x_1, x_2, ..., x_N) = F_0 + \sum \lambda_i \bar{x}_i^{\,2} \tag{3}$$

where λ_i are the eigenvalues of the matrix H_{ij} (The barred new variables in Eq. (3) are measured along the eigenvectors of H_{ij}).

The number of negative eigenvalues in Eq. (3) is the so-called Morse index. A negative eigenvalue means that along the corresponding eigenvector the critical point is a maximum and a positive eigenvalue means a minimum along the corresponding direction. Local minima have Morse index (MI) of 0, local maxima have MI of N and saddle points have MI between 1 and N-1.

For the network structure it is sufficient to consider saddle points with MI = 1, i.e. saddle points that are maxima along one direction. From such a saddle point, two distinct local minima can be generated by letting the optimization go down on its two sides along that direction. The optimization paths, together with the saddle point with MI = 1, form a link in the optimization space between the two minima. The local minima that are connected together in this way form a network.

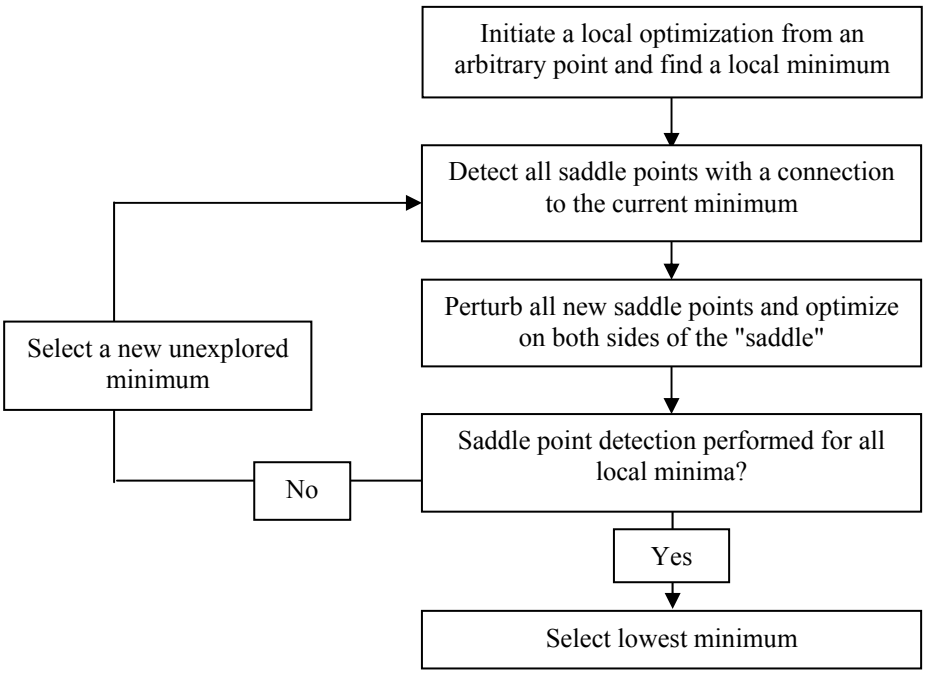

Fig. 1: Flow chart for the network global search method.

A network global search method (see Fig. 1) based on the saddle point detection has been developed[5-7]. For a given local minimum, the algorithm detects all saddle points with MI = 1 that are connected with it. Via local optimization performed on both sides of each saddle point, two minima are obtained. At each new minimum a saddle point search is performed to find the remaining part of the network. At the last stage the best solutions (i.e. the solutions for which the imaging quality is satisfactory) are selected.

The algorithm has been implemented in our program NETMIN, which for local optimization calls the commercial optical design program CODE V. The two programs communicate via the operating system.

3. TOPOGRAPHY OF THE MERIT FUNCTION SPACE OF EUV MIRROR SYSTEMS

We have used the algorithm described above on several EUV ring-field configurations that consist of four, six or eight mirrors. In this article, we present results of the network global search for a six-mirror configuration (Fig. 2). Since for EUV systems with high-order aspheric surfaces in certain domains of the merit function space even local optimization tends to become unstable[8], we did not attempt to detect the entire network, but we focused on regions of interest in stable domains of the merit function space. All surfaces are aspheric, with aspheric coefficients going up to the 10^{th} order on each surface. However, because network explorations with all variables (37 in this case: 6 curvatures + 24 aspheres + 7 distances) is very time consuming, in all our searches only the six surface curvatures have been used as variables, while the aspheric coefficients have been kept constant with non zero values. (Curvatures generate much more local minima than distances and aspheric coefficients.) The default CODE V merit function, which is based on transverse aberrations, has been used.

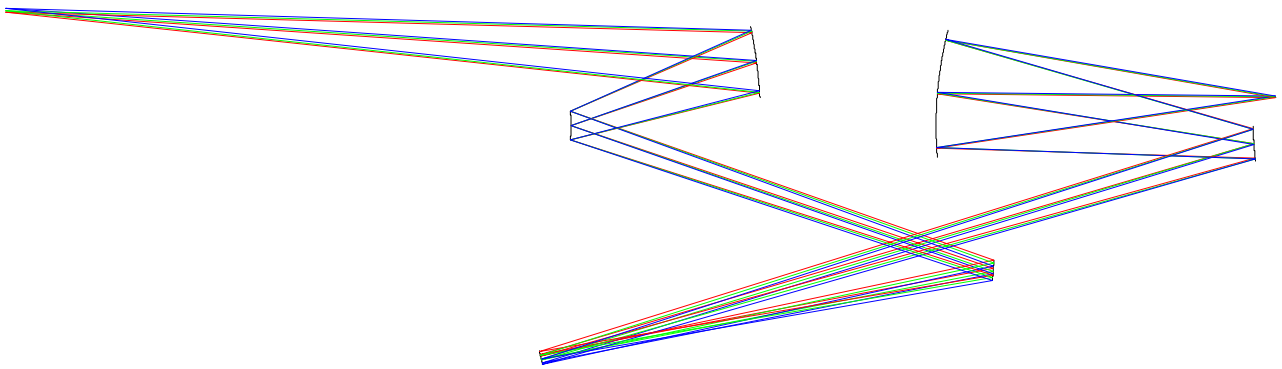

Fig. 2: Six-mirror microlithographic projection system with object heights between 114 and 118 mm, a numerical aperture of 0.16 and a magnification of 0.25.

In our research, we have followed two directions. We have analyzed the change in the merit function space when:

a) control parameters, such as numerical aperture and field, are modified;
b) at fixed values of numerical aperture and field, constraints, such as telecentricity at the image plane, quasi-telecentricity at the object plane, freedom of obstruction, distortion within certain limits, are used to limit the variation domain of the variables.

3.1 Influence of the control parameters on the merit function space of EUV mirror systems

In our first example, we discuss the topography of the merit function space of the six-mirror system presented in Fig. 2. The system has been constrained to be paraxially telecentric on the image side, i.e. the paraxial chief ray leaving the last mirror must be parallel to the optical axis. The magnification was kept at a constant value of 0.25. A region of interest in the network, as detected with the present version of NETMIN, is presented in Fig. 3. In this graph each node represents either a local minimum or a saddle point with MI = 1 in the merit function space and the lines connecting the nodes show to which minima the optimization paths that start at saddle points go. This graph allows us to determine the relationships between different local minima independently of the dimensionality of the merit function space.

The part of the network presented in Fig. 3 provides useful information. For example, we observe that in addition to the minimum with the lowest merit function (m10.8575), there are two other solutions in this space that have good performances, i.e. low values of the merit function. These two solutions and the best minimum are underlined in Fig. 3. The three solutions are connected via saddle points that have slightly higher values of the merit function. Therefore, along the entire network path between these three solutions in the merit function space, the variations of the merit function are very small (as compared to the variations in the rest of the network).

The connections between the best systems in the network and the fact that outside the region where they were found the merit function increases drastically, support Isshiki's conjecture according to which the minima with nearly the lowest merit function are situated in a string winding through the merit function space[9].

Analyzing the remaining configurations, we observe that they are situated either in an obstructed space (at this stage freedom of obstruction has not been imposed as constraint) or in a space where they are not real telecentric at the wafer side (i.e. because of aberrations the real chief ray deviates from the paraxial one and is not parallel to the optical axis). As mentioned above, here we have imposed the paraxial telecentricity constraint. For instance, the unobstructed saddle point s738.994 (underlined with a dotted line) that connects the unobstructed local minimum m565.349 with the obstructed m24.8711.

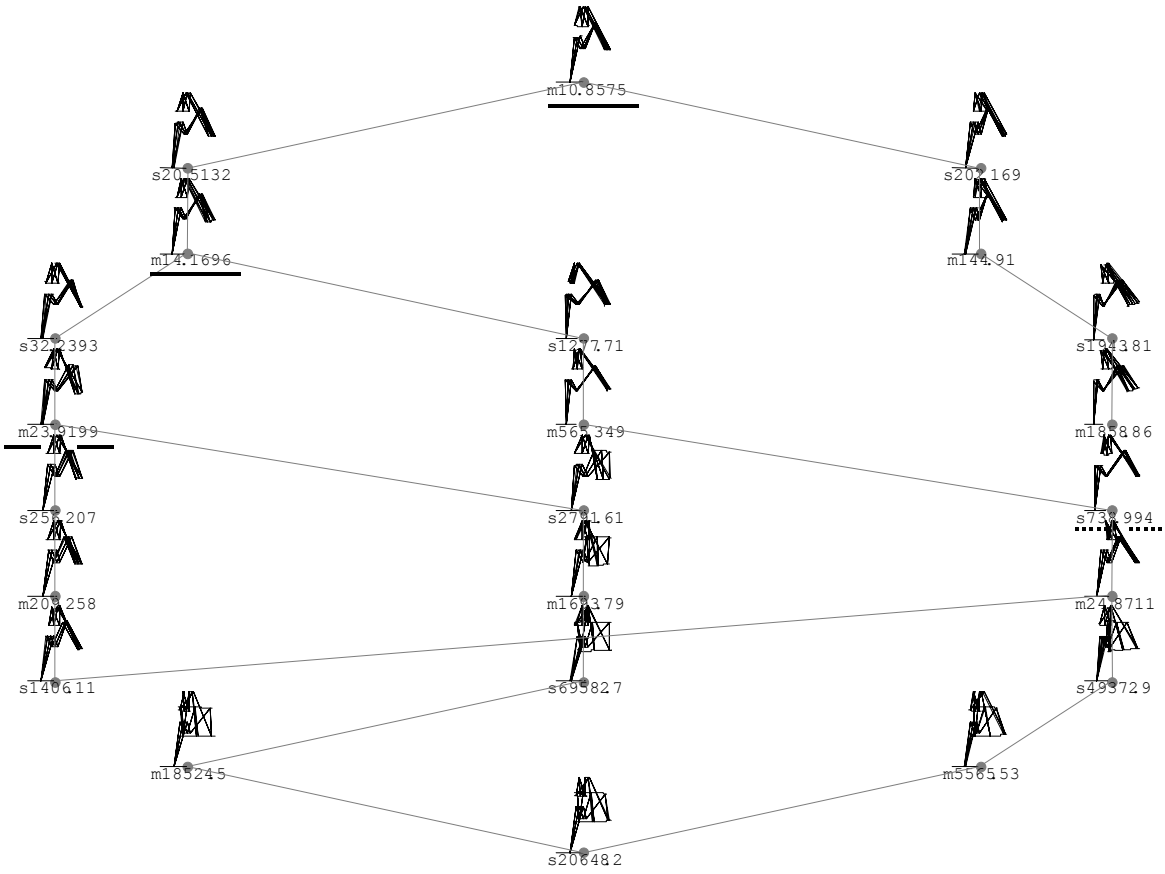

Fig. 3: Network structure of a six-mirror system search corresponding to the system shown in Fig. 2. S represents saddle points. M represents minima. The value of the merit function is also shown.

When we reduce the numerical aperture and the field with one third, our algorithm finds the network shown in Fig. 4. Again, three solutions (underlined in Fig. 4) having the best performance are observed. If we reset the numerical aperture and the field of these three solutions to their initial values and then we locally reoptimize them, we observe that they converge to the three best solutions in Fig. 3: m1.23439 becomes m23.9199, m5.10904 becomes m14.1696 and m1.70821 becomes m10.8575. The best minimum at low numerical aperture and field (m1.23439) is not anymore the best minimum when the values of these control parameters are increased. However, it is still one of the good solutions obtained.

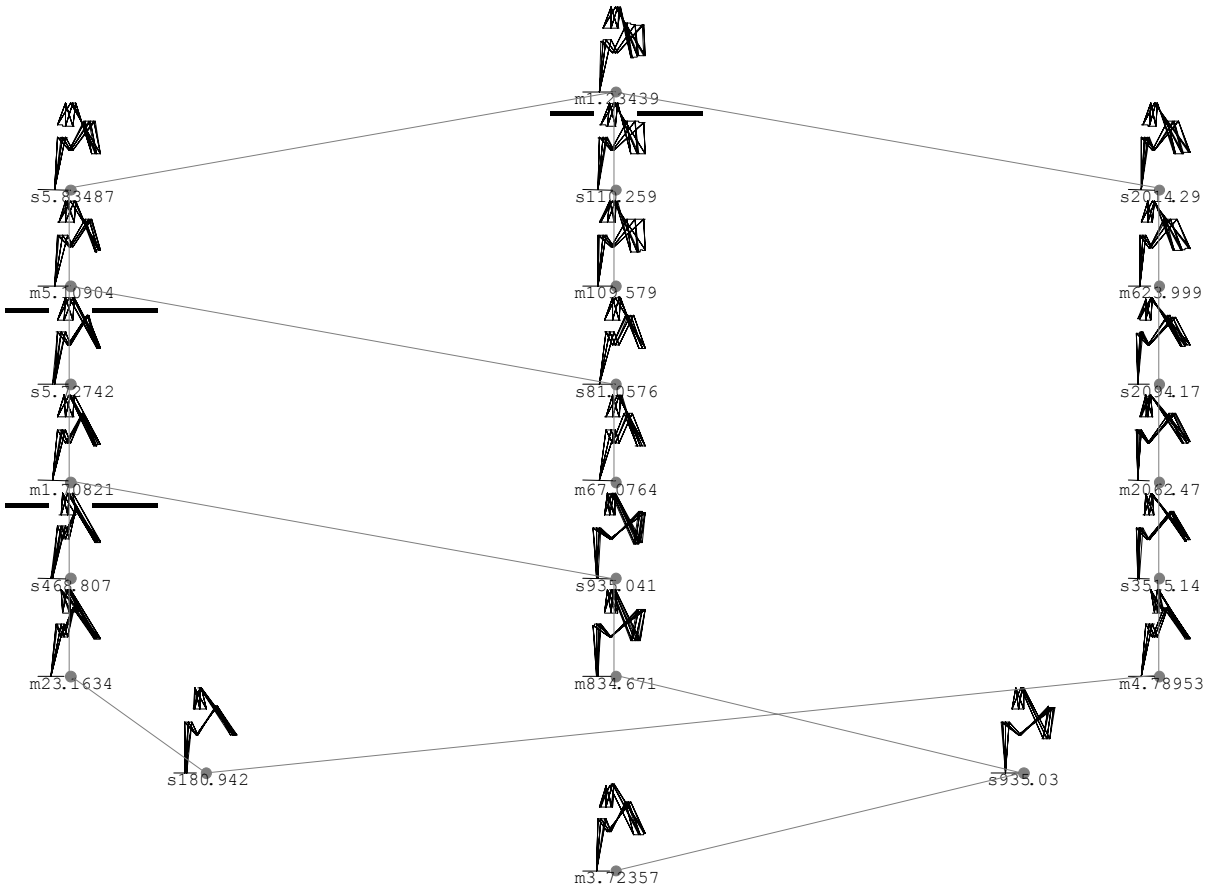

Fig. 4: Network structure of the merit function space of a six-mirror system having reduced numerical aperture and field.

We have made several network runs for the six-mirror system with different values of the control parameters. Comparing the results we observed that small changes in the control parameters do not change the networks significantly. However, when the changes are large, parts of the networks tend to appear or disappear. For instance, two minima and a saddle point in between (m1.23439, m109.579 and s110.259 in Fig. 4) found at low numerical aperture and field become a single minimum (m23.9199 in Fig. 3) once the values of the two parameters are increased. The network structure (i.e. the number of nodes and the connections between them) changes, however, the best solutions remain in the structurally stable part of the network. (In fact, a similar behavior is observed for many other types of systems. For instance, for the Cooke Triplet, if the aperture is low enough, we have two minima having the well-known Cooke Triplet shape and a saddle point between them, but when the aperture is increased beyond a threshold value, only one minimum remains[10]).

3.2. The influence of constraints on the merit function space of EUV mirror systems

We have also analyzed the merit function space of the same six-mirror system (Fig. 2), but with different constraints. For instance, we have changed the conditions in which we have found the network shown in Fig. 3, replacing the paraxial telecentricity with real telecentricity, i.e. the real chief ray at the wafer stage must be parallel to the optical axis.

Despite significant differences in the network (Fig. 5), which are either real or caused by the limitations of the present version of NETMIN, the three good solutions mentioned earlier are found again. When optimizing them in a space constrained by paraxial telecentricity at the image plane they converge to the three best solutions of the network detected under these conditions: the local minimum m15.0369 in Fig. 5 goes to m14.1696 in Fig. 3 and local minimum m33.927 goes to m23.9199. Interestingly, the best minimum m8.77179 corresponds to the best minimum in Fig. 3.

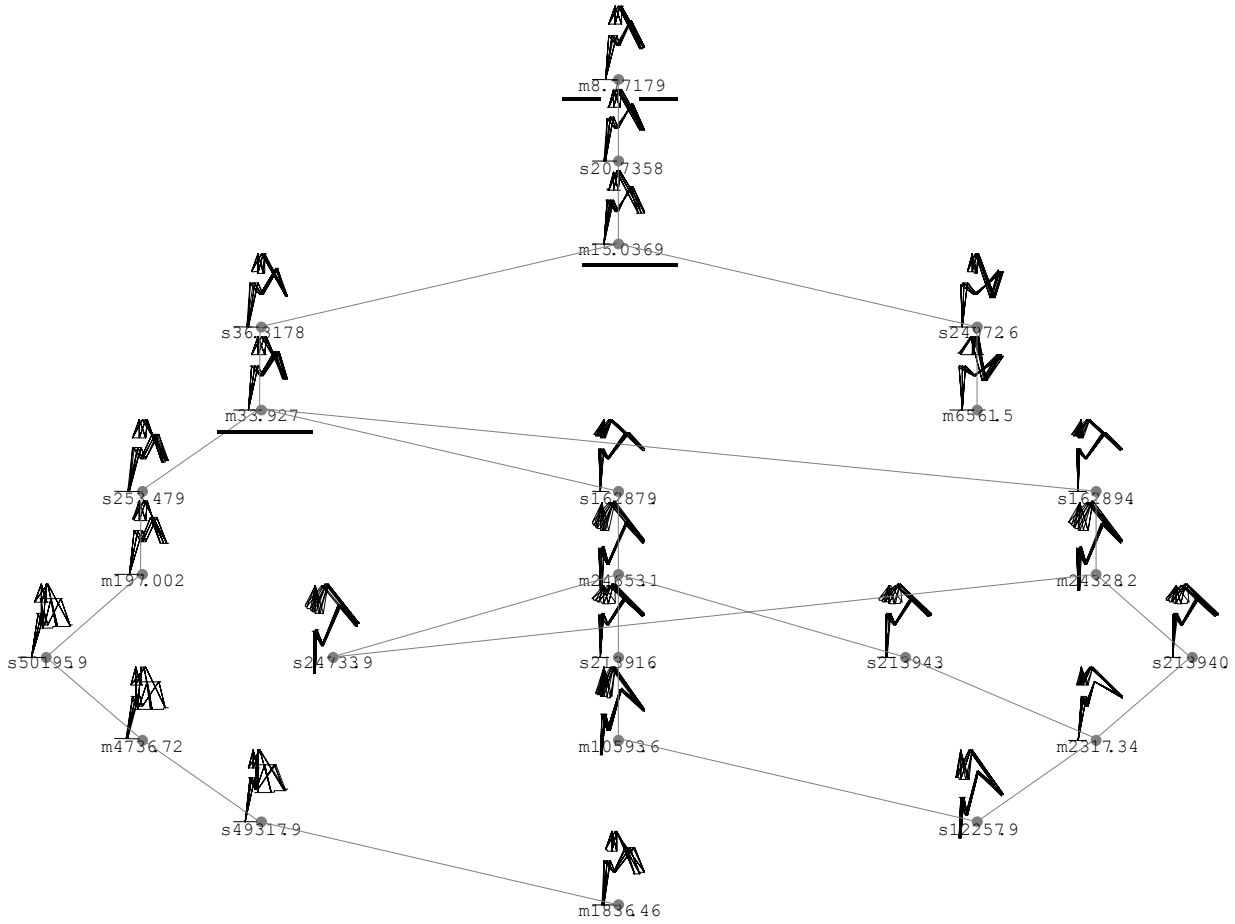

Fig. 5: Network structure of a six-mirror system search with real telecentricity in the image space.

Such network analyses have also been made by using other constraints related to paraxial and real quasi-telecentricity on the object side (i.e. the upper paraxial, respectively real marginal ray must be parallel to the optical axis), freedom of obstruction and distortion. Because we had only six variables we did not use all of them at the same time, but we used different combinations of them.

In addition to the merit function space of the system presented in Fig. 2, we have studied the merit function space of a number of six-mirror systems having different configurations, as well as for a four- and some eight- mirror systems. In virtually all cases we have studied we have observed that, when constraints are modified, the same system remains the best one (i.e. after reoptimization the best system in one run becomes the best system in the other run). Surprisingly, this happens even when distortion is controlled (within limits that were not very tight), but we believe that this result is specific to our systems. For other types of systems, distortion control may change the system.

4. FULLY OPTIMIZED DESIGN

Finally, from a network run very similar to those in Figs. 3 and 5, the system that corresponds to the best minimum in Fig. 5 has been optimized traditionally, with all variables and using practical requirements. The result is shown in Fig. 6 and some of the system's specifications and performances are shown in Table 1. All surfaces are aspheric. The aperture stop is situated at the second mirror. Distortion is kept below 1 nm per field. The system is unobstructed. The angle of incidence of the chief ray at the mask takes a value of approximately 4.4°. At the wafer side the system is telecentric, i.e. the chief ray is (approximately) perpendicular on the image plane. For multilayer compatibility the angles of incidence of the chief ray at each surface ("Angle" in Table 1) have been kept smaller than 20°, five of them below 13°.

		Mirror	Angle
NA	0.25		
Field	114 .. 118 mm	1	12.17°
Wavelength	13 nm	2	20°
Magnification	0.25	3	11.62°
Distortion	< 1 nm	4	6.88°
Strehl ratio	0.995	5	12.88°
Wavefront aberration	0.016 λ	6	4.39°

Table 1: Specifications for the optimized EUV mirror system presented in Fig. 6.

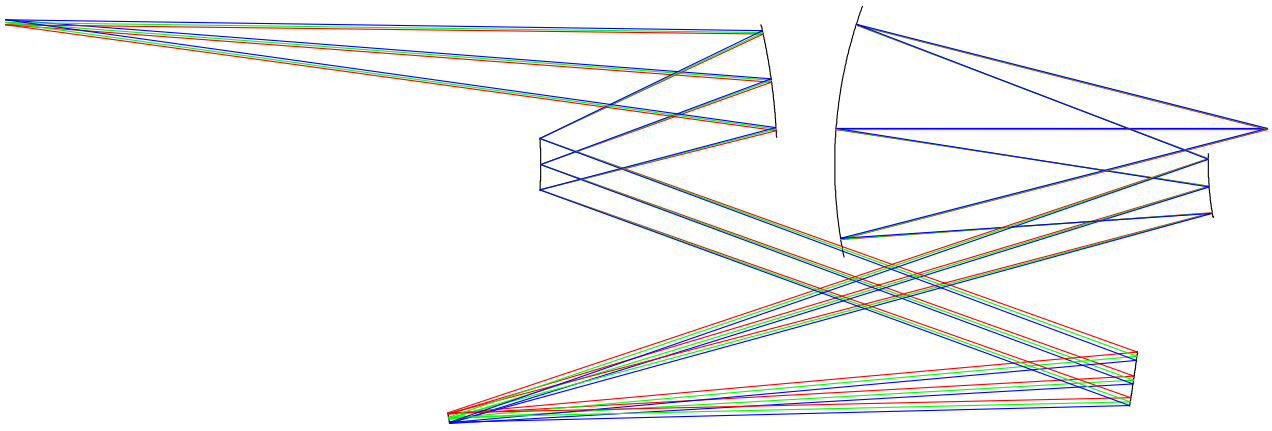

Fig. 6: Six-mirror projection system for EUV lithography.

5. CONCLUSIONS

We have shown that the idea that local minima form a network can be used for practical purposes for complex systems such as the EUV mirror systems.

When control parameters are modified, the network structure changes, but the good systems tend to remain nodes in the network. When, at constant values of the numerical aperture and field, constraints are modified, the same node in the network corresponds to the best minimum.

We have also shown that a relaxed use of constraints in the network search is sufficient for the purpose of generating starting points for further traditional local optimization. Moreover, we have shown that starting from a solution found by our network detection algorithm in a low-dimensional search, we have obtained a high-quality six-mirror system with performances that make it suitable for practical applications.

6. ACKNOWLEDGEMENTS

The first author gratefully acknowledges the financial support of ASLM. We also thank Eco van Driel for programming NETMIN.

7. REFERENCES

1. T. G. Kuper, T. I. Harris, "Global optimization for lens design - an emerging technology", *Proc. SPIE* **1780**, 14-28, 1992
2. M. Isshiki, H. Ono, K. Hiraga, J. Ishikawa, S. Nakadate, "Lens design: Global optimization with Escape Function", *Optical Review* (Japan) **6**, 463-470, 1995
3. G. W. Forbes, A. E. W. Jones, "Towards global optimization with adaptive simulated annealing", *Proc. SPIE* **1354**, 144-151, 1991
4. K.E. Moore, "Algorithm for global optimization of optical systems based on genetic competition", *Proc. SPIE* **3780**, 40-47, 1999
5. F. Bociort, E. van Driel, A. Serebriakov, "Networks of local minima in optical system optimization", *Optics Letters* **29**(2), 189-191, 2004
6. E. van Driel, F. Bociort, A. Serebriakov, "Topography of the merit function landscape in optical system design", *Proc. SPIE* **5249**, 353-363, 2004
7. F. Bociort, A. Serebriakov, M. van Turnhout, "Saddle points in the merit function landscape of systems of thin lenses in contact", *Proc. SPIE* **5523**, 174-184, 2004
8. O. Marinescu, F. Bociort, J. Braat, "Avoiding unstable regions in the design space of EUV mirror systems comprising high-order aspheric surfaces", *Proc. SPIE* **5523**, 185-192, 2004
9. M. Isshiki, L. Gardner, G.G. Gregory, "Automated control of manufacturing sensitivity during optimization", *Proc. SPIE* **5249**, 343-352, 2004
10. F. Bociort, E. van Driel, A. Serebriakov, "Network structure of the set of local minima in optical system optimization", Proc. *SPIE* **5174**, 26-34, 2003